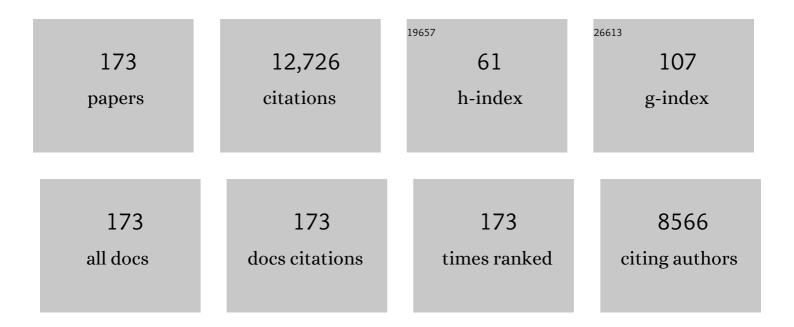
## List of Publications by Year in descending order

Source: https://exaly.com/author-pdf/7122589/publications.pdf Version: 2024-02-01



#	Article	IF	CITATIONS
1	Lightweight conductive graphene/thermoplastic polyurethane foams with ultrahigh compressibility for piezoresistive sensing. Journal of Materials Chemistry C, 2017, 5, 73-83.	5.5	576
2	Electrically conductive polymer composites for smart flexible strain sensors: a critical review. Journal of Materials Chemistry C, 2018, 6, 12121-12141.	5.5	522
3	Electrically conductive thermoplastic elastomer nanocomposites at ultralow graphene loading levels for strain sensor applications. Journal of Materials Chemistry C, 2016, 4, 157-166.	5.5	484
4	Electrically conductive strain sensing polyurethane nanocomposites with synergistic carbon nanotubes and graphene bifillers. Nanoscale, 2016, 8, 12977-12989.	5.6	464
5	Continuously prepared highly conductive and stretchable SWNT/MWNT synergistically composited electrospun thermoplastic polyurethane yarns for wearable sensing. Journal of Materials Chemistry C, 2018, 6, 2258-2269.	5.5	376
6	Flexible electrically resistive-type strain sensors based on reduced graphene oxide-decorated electrospun polymer fibrous mats for human motion monitoring. Carbon, 2018, 126, 360-371.	10.3	367
7	The effect of filler dimensionality on the electromechanical performance of polydimethylsiloxane based conductive nanocomposites for flexible strain sensors. Composites Science and Technology, 2017, 139, 64-73.	7.8	300
8	A highly stretchable and stable strain sensor based on hybrid carbon nanofillers/polydimethylsiloxane conductive composites for large human motions monitoring. Composites Science and Technology, 2018, 156, 276-286.	7.8	276
9	Significant Stretchability Enhancement of a Crack-Based Strain Sensor Combined with High Sensitivity and Superior Durability for Motion Monitoring. ACS Applied Materials & Interfaces, 2019, 11, 7405-7414.	8.0	243
10	Carbon Nanotubes-Adsorbed Electrospun PA66 Nanofiber Bundles with Improved Conductivity and Robust Flexibility. ACS Applied Materials & Interfaces, 2016, 8, 14150-14159.	8.0	241
11	Comparative assessment of the strain-sensing behaviors of polylactic acid nanocomposites: reduced graphene oxide or carbon nanotubes. Journal of Materials Chemistry C, 2017, 5, 2318-2328.	5.5	236
12	Lightweight and Robust Carbon Nanotube/Polyimide Foam for Efficient and Heat-Resistant Electromagnetic Interference Shielding and Microwave Absorption. ACS Applied Materials & Interfaces, 2020, 12, 8704-8712.	8.0	227
13	Flexible and Lightweight Pressure Sensor Based on Carbon Nanotube/Thermoplastic Polyurethane-Aligned Conductive Foam with Superior Compressibility and Stability. ACS Applied Materials & Interfaces, 2017, 9, 42266-42277.	8.0	225
14	Ultra-Stretchable, durable and conductive hydrogel with hybrid double network as high performance strain sensor and stretchable triboelectric nanogenerator. Nano Energy, 2020, 76, 105035.	16.0	209
15	Organic vapor sensing behaviors of conductive thermoplastic polyurethane–graphene nanocomposites. Journal of Materials Chemistry C, 2016, 4, 4459-4469.	5.5	198
16	Asymmetric conductive polymer composite foam for absorption dominated ultra-efficient electromagnetic interference shielding with extremely low reflection characteristics. Journal of Materials Chemistry A, 2020, 8, 9146-9159.	10.3	196
17	Electrically conductive carbon black (CB) filled in situ microfibrillar poly(ethylene terephthalate) (PET)/polyethylene (PE) composite with a selective CB distribution. Polymer, 2007, 48, 849-859.	3.8	194
18	Highly stretchable and durable strain sensor based on carbon nanotubes decorated thermoplastic polyurethane fibrous network with aligned wave-like structure. Chemical Engineering Journal, 2019, 360, 762-777.	12.7	190

#	Article	IF	CITATIONS
19	Environment Tolerant Conductive Nanocomposite Organohydrogels as Flexible Strain Sensors and Power Sources for Sustainable Electronics. Advanced Functional Materials, 2021, 31, 2101696.	14.9	179
20	Ultra-stretchable triboelectric nanogenerator as high-sensitive and self-powered electronic skins for energy harvesting and tactile sensing. Nano Energy, 2020, 70, 104546.	16.0	171
21	A comparison between strain sensing behaviors of carbon black/polypropylene and carbon nanotubes/polypropylene electrically conductive composites. Composites Part A: Applied Science and Manufacturing, 2013, 48, 129-136.	7.6	159
22	Electrically conductive thermoplastic polyurethane/polypropylene nanocomposites with selectively distributed graphene. Polymer, 2016, 97, 11-19.	3.8	159
23	Conductive thermoplastic polyurethane composites with tunable piezoresistivity by modulating the filler dimensionality for flexible strain sensors. Composites Part A: Applied Science and Manufacturing, 2017, 101, 41-49.	7.6	155
24	Flexible and wearable carbon black/thermoplastic polyurethane foam with a pinnate-veined aligned porous structure for multifunctional piezoresistive sensors. Chemical Engineering Journal, 2020, 382, 122985.	12.7	153
25	Superhydrophobic Shish-kebab Membrane with Self-Cleaning and Oil/Water Separation Properties. ACS Sustainable Chemistry and Engineering, 2018, 6, 9866-9875.	6.7	147
26	Multifunctional flexible carbon black/polydimethylsiloxane piezoresistive sensor with ultrahigh linear range, excellent durability and oil/water separation capability. Chemical Engineering Journal, 2019, 372, 373-382.	12.7	146
27	Smart strain sensing organic–inorganic hybrid hydrogels with nano barium ferrite as the cross-linker. Journal of Materials Chemistry C, 2019, 7, 2353-2360.	5.5	142
28	A Highly Sensitive and Stretchable Yarn Strain Sensor for Human Motion Tracking Utilizing a Wrinkle-Assisted Crack Structure. ACS Applied Materials & Interfaces, 2019, 11, 36052-36062.	8.0	141
29	Ultra-stretchable, sensitive and durable strain sensors based on polydopamine encapsulated carbon nanotubes/elastic bands. Journal of Materials Chemistry C, 2018, 6, 8160-8170.	5.5	131
30	A highly stretchable carbon nanotubes/thermoplastic polyurethane fiber-shaped strain sensor with porous structure for human motion monitoring. Composites Science and Technology, 2018, 168, 126-132.	7.8	127
31	High-Performance Wearable Strain Sensor Based on Graphene/Cotton Fabric with High Durability and Low Detection Limit. ACS Applied Materials & Interfaces, 2020, 12, 1474-1485.	8.0	125
32	Ultralight carbon nanotube/graphene/polyimide foam with heterogeneous interfaces for efficient electromagnetic interference shielding and electromagnetic wave absorption. Carbon, 2021, 176, 118-125.	10.3	122
33	Flexible conductive polymer composites for smart wearable strain sensors. SmartMat, 2020, 1, e1010.	10.7	119
34	Highly Stretchable and Sensitive Strain Sensor with Porous Segregated Conductive Network. ACS Applied Materials & Interfaces, 2019, 11, 37094-37102.	8.0	116
35	Bioinspired Multifunctional Photonicâ€Electronic Smart Skin for Ultrasensitive Health Monitoring, for Visual and Selfâ€Powered Sensing. Advanced Materials, 2021, 33, e2102332.	21.0	107
36	Multifunctional stretchable strain sensor based on polydopamine/ reduced graphene oxide/ electrospun thermoplastic polyurethane fibrous mats for human motion detection and environment monitoring. Composites Part B: Engineering, 2020, 183, 107696.	12.0	104

#	Article	IF	CITATIONS
37	Piezoresistive behavior of porous carbon nanotube-thermoplastic polyurethane conductive nanocomposites with ultrahigh compressibility. Applied Physics Letters, 2016, 108, .	3.3	102
38	A super-stretchable and tough functionalized boron nitride/PEDOT:PSS/poly( <i>N</i> -isopropylacrylamide) hydrogel with self-healing, adhesion, conductive and photothermal activity. Journal of Materials Chemistry A, 2019, 7, 8204-8209.	10.3	101
39	A flexible and self-formed sandwich structure strain sensor based on AgNW decorated electrospun fibrous mats with excellent sensing capability and good oxidation inhibition properties. Journal of Materials Chemistry C, 2017, 5, 7035-7042.	5.5	100
40	Conductive herringbone structure carbon nanotube/thermoplastic polyurethane porous foam tuned by epoxy for high performance flexible piezoresistive sensor. Composites Science and Technology, 2017, 149, 166-177.	7.8	99
41	A tunable strain sensor based on a carbon nanotubes/electrospun polyamide 6 conductive nanofibrous network embedded into poly(vinyl alcohol) with self-diagnosis capabilities. Journal of Materials Chemistry C, 2017, 5, 4408-4418.	5.5	98
42	Low-temperature carbonized carbon nanotube/cellulose aerogel for efficient microwave absorption. Composites Part B: Engineering, 2021, 220, 108985.	12.0	95
43	Strain sensing behaviors of epoxy nanocomposites with carbon nanotubes under cyclic deformation. Polymer, 2017, 112, 1-9.	3.8	94
44	Design of Helically Double-Leveled Gaps for Stretchable Fiber Strain Sensor with Ultralow Detection Limit, Broad Sensing Range, and High Repeatability. ACS Applied Materials & Interfaces, 2019, 11, 4345-4352.	8.0	91
45	Facile fabrication of triboelectric nanogenerator based on low-cost thermoplastic polymeric fabrics for large-area energy harvesting and self-powered sensing. Nano Energy, 2019, 65, 104068.	16.0	89
46	Superior and highly absorbed electromagnetic interference shielding performance achieved by designing the reflection-absorption-integrated shielding compartment with conductive wall and lossy core. Chemical Engineering Journal, 2020, 393, 124644.	12.7	87
47	Ultra-sensitive and durable strain sensor with sandwich structure and excellent anti-interference ability for wearable electronic skins. Composites Science and Technology, 2020, 200, 108448.	7.8	85
48	Continuous fabrication of polymer microfiber bundles with interconnected microchannels for oil/water separation. Applied Materials Today, 2017, 9, 77-81.	4.3	84
49	Ultrastretchable Multilayered Fiber with a Hollow-Monolith Structure for High-Performance Strain Sensor. ACS Applied Materials & Interfaces, 2018, 10, 34592-34603.	8.0	81
50	Highly stretchable and durable fiber-shaped strain sensor with porous core-sheath structure for human motion monitoring. Composites Science and Technology, 2020, 189, 108038.	7.8	81
51	Self-assembled reduced graphene oxide/nickel nanofibers with hierarchical core-shell structure for enhanced electromagnetic wave absorption. Carbon, 2020, 167, 530-540.	10.3	80
52	Continuously fabricated transparent conductive polycarbonate/carbon nanotube nanocomposite films for switchable thermochromic applications. Journal of Materials Chemistry C, 2018, 6, 8360-8371.	5.5	79
53	Electrical conductivity and major mechanical and thermal properties of carbon nanotubeâ€filled polyurethane foams. Journal of Applied Polymer Science, 2011, 120, 3014-3019.	2.6	77
54	Aligned flexible conductive fibrous networks for highly sensitive, ultrastretchable and wearable strain sensors. Journal of Materials Chemistry C, 2018, 6, 6575-6583.	5.5	77

#	Article	IF	CITATIONS
55	Ultrathin, flexible transparent Joule heater with fast response time based on single-walled carbon nanotubes/poly(vinyl alcohol) film. Composites Science and Technology, 2019, 183, 107796.	7.8	77
56	Highly Stretchable, Transparent, and Bioâ€Friendly Strain Sensor Based on Selfâ€Recovery Ionicâ€Covalent Hydrogels for Human Motion Monitoring. Macromolecular Materials and Engineering, 2019, 304, 1900227.	3.6	71
57	Remarkably anisotropic conductive MWCNTs/polypropylene nanocomposites with alternating microlayers. Chemical Engineering Journal, 2019, 358, 924-935.	12.7	70
58	Mechanical enhancement of melt-stretched β-nucleated isotactic polypropylene: The role of lamellar branching of β-crystal. Polymer Testing, 2017, 58, 227-235.	4.8	69
59	Tunable and Nacreâ€Mimetic Multifunctional Electronic Skins for Highly Stretchable Contactâ€Noncontact Sensing. Small, 2021, 17, e2100542.	10.0	69
60	Heating-induced negative temperature coefficient effect in conductive graphene/polymer ternary nanocomposites with a segregated and double-percolated structure. Journal of Materials Chemistry C, 2017, 5, 8233-8242.	5.5	66
61	Ultra-stretchable and multifunctional wearable electronics for superior electromagnetic interference shielding, electrical therapy and biomotion monitoring. Journal of Materials Chemistry A, 2021, 9, 7238-7247.	10.3	65
62	Tuning of vapor sensing behaviors of eco-friendly conductive polymer composites utilizing ramie fiber. Sensors and Actuators B: Chemical, 2015, 221, 1279-1289.	7.8	64
63	Ultraâ€Stretchable Porous Fiberâ€Shaped Strain Sensor with Exponential Response in Full Sensing Range and Excellent Antiâ€Interference Ability toward Buckling, Torsion, Temperature, and Humidity. Advanced Electronic Materials, 2019, 5, 1900538.	5.1	63
64	A Healable and Mechanically Enhanced Composite with Segregated Conductive Network Structure for High-Efficient Electromagnetic Interference Shielding. Nano-Micro Letters, 2021, 13, 162.	27.0	62
65	Hollow-porous fibers for intrinsically thermally insulating textiles and wearable electronics with ultrahigh working sensitivity. Materials Horizons, 2021, 8, 1037-1046.	12.2	59
66	Electrically conductive in situ microfibrillar composite with a selective carbon black distribution: An unusual resistivity–temperature behavior upon cooling. Polymer, 2008, 49, 1037-1048.	3.8	58
67	Crystalline Structure of Injection Molded $\hat{l}^2$ -Isotactic Polypropylene: Analysis of the Oriented Shear Zone. Industrial & amp; Engineering Chemistry Research, 2013, 52, 11996-12002.	3.7	58
68	Segregated conductive polymer composite with synergistically electrical and mechanical properties. Composites Part A: Applied Science and Manufacturing, 2018, 105, 68-77.	7.6	55
69	Interfacial interaction enhancement by shear-induced β-cylindrite in isotactic polypropylene/glass fiber composites. Polymer, 2016, 100, 111-118.	3.8	54
70	Multifunctional interlocked e-skin based on elastic micropattern array facilely prepared by hot-air-gun. Chemical Engineering Journal, 2021, 407, 127960.	12.7	54
71	Facile heteroatom doping of biomass-derived carbon aerogels with hierarchically porous architecture and hybrid conductive network: Towards high electromagnetic interference shielding effectiveness and high absorption coefficient. Composites Part B: Engineering, 2021, 224, 109175.	12.0	50
72	Vapor sensing performance as a diagnosis probe to estimate the distribution of multi-walled carbon nanotubes in poly(lactic acid)/polypropylene conductive composites. Sensors and Actuators B: Chemical, 2018, 255, 2809-2819.	7.8	41

#	Article	IF	CITATIONS
73	An electrically conductive polymer composite with a co-continuous segregated structure for enhanced mechanical performance. Journal of Materials Chemistry C, 2020, 8, 11546-11554.	5.5	40
74	Morphological comparison of isotactic polypropylene molded by water-assisted and conventional injection molding. Journal of Materials Science, 2011, 46, 7830-7838.	3.7	39
75	Electrically conductive carbon black/electrospun polyamide 6/poly(vinyl alcohol) composite based strain sensor with ultrahigh sensitivity and favorable repeatability. Materials Letters, 2019, 236, 60-63.	2.6	39
76	Highly Thermally Conductive Graphene-Based Thermal Interface Materials with a Bilayer Structure for Central Processing Unit Cooling. ACS Applied Materials & Interfaces, 2021, 13, 25325-25333.	8.0	39
77	Nacre-inspired tunable strain sensor with synergistic interfacial interaction for sign language interpretation. Nano Energy, 2021, 90, 106606.	16.0	39
78	Annealing Induced Mechanical Reinforcement of Injection Molded iPP Parts. Macromolecular Materials and Engineering, 2016, 301, 1468-1472.	3.6	38
79	Highly enhanced microwave absorption for carbon nanotube/barium ferrite composite with ultra-low carbon nanotube loading. Journal of Materials Science and Technology, 2022, 102, 115-122.	10.7	37
80	Anomalous attenuation of the positive temperature coefficient of resistivity in a carbon-black-filled polymer composite with electrically conductive in situ microfibrils. Applied Physics Letters, 2006, 89, 032105.	3.3	36
81	Tuning of liquid sensing performance of conductive carbon black (CB)/polypropylene (PP) composite utilizing a segregated structure. Composites Part A: Applied Science and Manufacturing, 2013, 55, 11-18.	7.6	36
82	Wide distribution of shish-kebab structure and tensile property of micro-injection-molded isotactic polypropylene microparts: a comparative study with injection-molded macroparts. Journal of Materials Science, 2014, 49, 1041-1048.	3.7	36
83	Steric stabilizer-based promotion of uniform polyaniline shell for enhanced electromagnetic wave absorption of carbon nanotube/polyaniline hybrids. Composites Part B: Engineering, 2020, 199, 108309.	12.0	36
84	Multi-functional and flexible helical fiber sensor for micro-deformation detection, temperature sensing and ammonia gas monitoring. Composites Part B: Engineering, 2021, 211, 108621.	12.0	35
85	Stretchable, Sensitive Strain Sensors with a Wide Workable Range and Low Detection Limit for Wearable Electronic Skins. ACS Applied Materials & Interfaces, 2022, 14, 4562-4570.	8.0	35
86	Interface and electronic structure engineering induced Prussian blue analogues with ultra-stable capability for aqueous NH <sub>4</sub> <sup>+</sup> storage. Nanoscale, 2022, 14, 8501-8509.	5.6	35
87	Synergistic effect of carbon fibers on the conductive properties of a segregated carbon black/polypropylene composite. Materials Letters, 2014, 129, 72-75.	2.6	33
88	Highly linear and low hysteresis porous strain sensor for wearable electronic skins. Composites Communications, 2021, 26, 100809.	6.3	33
89	Tuning of the PTC and NTC effects of conductive CB/PA6/HDPE composite utilizing an electrically superfine electrospun network. Materials Letters, 2014, 132, 48-51.	2.6	32
90	Shear-induced interfacial sheath structure in isotactic polypropylene/glass fiber composites. Polymer, 2015, 70, 326-335.	3.8	32

#	Article	IF	CITATIONS
91	Temperature-resistivity characteristics of a segregated conductive CB/PP/UHMWPE composite. Colloid and Polymer Science, 2014, 292, 2891-2898.	2.1	30
92	Positive Temperature Coefficient (PTC) Evolution of Segregated Structural Conductive Polypropylene Nanocomposites with Visually Traceable Carbon Black Conductive Network. Advanced Materials Interfaces, 2017, 4, 1700265.	3.7	30
93	Bridging the segregated structure in conductive polypropylene composites: An effective strategy to balance the sensitivity and stability of strain sensing performances. Composites Science and Technology, 2018, 163, 18-25.	7.8	30
94	Anisotropic Conductive Polymer Composites Based on High Density Polyethylene/Carbon Nanotube/Polyoxyethylene Mixtures for Microcircuits Interconnection and Organic Vapor Sensor. ACS Applied Nano Materials, 2019, 2, 3636-3647.	5.0	30
95	Spontaneous exfoliation and tailoring derived oxygen-riched porous carbon nanosheets for superior Li+ storage performance. Chemical Engineering Journal, 2020, 387, 124104.	12.7	30
96	Liquid sensing behaviors of conductive polypropylene composites containing hybrid fillers of carbon fiber and carbon black. Composites Part B: Engineering, 2016, 94, 45-51.	12.0	29
97	Organic vapor sensing behaviors of carbon black/poly (lactic acid) conductive biopolymer composite. Colloid and Polymer Science, 2013, 291, 2871-2878.	2.1	28
98	Continuous fabrication of polyethylene microfibrilar bundles for wearable personal thermal management fabric. Applied Surface Science, 2021, 549, 149255.	6.1	28
99	Flexible and heat-resistant carbon nanotube/graphene/polyimide foam for broadband microwave absorption. Composites Science and Technology, 2021, 212, 108848.	7.8	28
100	Positive temperature coefficient and timeâ€dependent resistivity of carbon nanotubes (CNTs)/ultrahigh molecular weight polyethylene (UHMWPE) composite. Journal of Applied Polymer Science, 2009, 114, 1002-1010.	2.6	27
101	Transparent Conductive Flexible Trilayer Films for a Deicing Window and Self-Recover Bending Sensor Based on a Single-Walled Carbon Nanotube/Polyvinyl Butyral Interlayer. ACS Applied Materials & Interfaces, 2020, 12, 1454-1464.	8.0	27
102	Highly stretchable and durable fibrous strain sensor with growth ring-like spiral structure for wearable electronics. Composites Part B: Engineering, 2021, 225, 109275.	12.0	27
103	Dual-functional thermal management materials for highly thermal conduction and effectively heat generation. Composites Part B: Engineering, 2022, 242, 110084.	12.0	27
104	Particle size induced tunable positive temperature coefficient characteristics in electrically conductive carbon nanotubes/polypropylene composites. Materials Letters, 2016, 182, 314-317.	2.6	26
105	Segregated conductive CNTs/HDPE/UHMWPE composites fabricated by plunger type injection molding. Materials Letters, 2018, 229, 13-16.	2.6	26
106	An Ultrasensitive, Durable and Stretchable Strain Sensor with Crack-wrinkle Structure for Human Motion Monitoring. Chinese Journal of Polymer Science (English Edition), 2021, 39, 316-326.	3.8	26
107	New insight into lamellar branching of β-nucleated isotactic polypropylene upon melt-stretching: WAXD and SAXS study. Journal of Materials Science, 2015, 50, 599-604.	3.7	25
108	Large-area fabrication and applications of patterned surface with anisotropic superhydrophobicity. Applied Surface Science, 2020, 529, 147027.	6.1	25

#	Article	IF	CITATIONS
109	Facile Construction of a Superhydrophobic Surface on a Textile with Excellent Electrical Conductivity and Stretchability. Industrial & Engineering Chemistry Research, 2020, 59, 7546-7553.	3.7	25
110	Anomalous attenuation and structural origin of positive temperature coefficient (PTC) effect in a carbon black (CB)/poly(ethylene terephthalate) (PET)/polyethylene (PE) electrically conductive microfibrillar polymer composite with a preferential CB distribution. Journal of Applied Polymer Science, 2012, 125, E561.	2.6	24
111	Realizing the simultaneously improved toughness and strength ofÂultra-thin LLDPE parts through annealing. Polymer, 2013, 54, 6843-6852.	3.8	24
112	Hierarchical nanofibrous mat via water-assisted electrospinning for self-powered ultrasensitive vibration sensors. Nano Energy, 2022, 97, 107149.	16.0	24
113	Pre-shear induced anomalous distribution of $\hat{I}^2$ -form in injection molded iPP. Polymer Testing, 2013, 32, 545-552.	4.8	23
114	Green Production of Covalently Functionalized Boron Nitride Nanosheets via Saccharide-Assisted Mechanochemical Exfoliation. ACS Sustainable Chemistry and Engineering, 2021, 9, 11155-11162.	6.7	23
115	Programmable micropatterned surface for single-layer homogeneous-polymer Janus actuator. Chemical Engineering Journal, 2022, 430, 133052.	12.7	23
116	Enhanced orientation of the waterâ€assisted injectionâ€molded ipp in the presence of nucleating agent. Polymer Engineering and Science, 2012, 52, 725-732.	3.1	22
117	Conductive network formation during annealing of an oriented polyethylene-based composite. Journal of Materials Science, 2012, 47, 3713-3719.	3.7	21
118	Unexpected molecular weight dependence of shish kebab in waterâ€assisted injection molded HDPE. Polymers for Advanced Technologies, 2013, 24, 270-272.	3.2	21
119	Interfacial adhesion enhanced flexible polycarbonate/carbon nanotubes transparent conductive film for vapor sensing. Composites Communications, 2019, 15, 80-86.	6.3	21
120	Building of multifunctional and hierarchical HxMoO3/PNIPAM hydrogel for high-efficiency solar vapor generation. Green Energy and Environment, 2022, 7, 1006-1013.	8.7	21
121	Bioinspired Concentric-Cylindrical Multilayered Scaffolds with Controllable Architectures: Facile Preparation and Biological Applications. ACS Applied Materials & Interfaces, 2018, 10, 43512-43522.	8.0	20
122	Amorphous MnSiO3 confined in graphene sheets for superior lithium-ion batteries. Journal of Alloys and Compounds, 2019, 804, 243-251.	5.5	20
123	Highly Stretchable Sheath–Core Yarns for Multifunctional Wearable Electronics. ACS Applied Materials & Interfaces, 2020, 12, 29717-29727.	8.0	20
124	Electrical Properties of an Ultralight Conductive Carbon Nanotube/Polymer Composite Foam Upon Compression. Polymer-Plastics Technology and Engineering, 2012, 51, 304-306.	1.9	19
125	The hierarchical structure of waterâ€essisted injection molded high density polyethylene: Small angle Xâ€ray scattering study. Journal of Applied Polymer Science, 2012, 125, 2297-2303.	2.6	19
126	Electrospun isotactic polypropylene fibers: Self-similar morphology and microstructure. Polymer, 2013, 54, 3117-3123.	3.8	19

#	Article	IF	CITATIONS
127	Enhancing oriented crystals in injection-molded HDPE through introduction of pre-shear. Materials & Design, 2015, 78, 12-18.	5.1	19
128	The strain-sensing behaviors of carbon black/polypropylene and carbon nanotubes/polypropylene conductive composites prepared by the vacuum-assisted hot compression. Colloid and Polymer Science, 2014, 292, 945-951.	2.1	18
129	Oriented structure in stretched isotactic polypropylene melt and its unexpected recrystallization: optical and Xâ€ray studies. Polymer International, 2011, 60, 1434-1441.	3.1	17
130	Nonlinear current-voltage characteristics of conductive polyethylene composites with carbon black filled pet microfibrils. Chinese Journal of Polymer Science (English Edition), 2013, 31, 211-217.	3.8	17
131	Thermo-compression-aligned functional graphene showing anisotropic response to in-plane stretching and out-of-plane bending. Journal of Materials Science, 2018, 53, 6574-6585.	3.7	17
132	Facile fabrication of highly durable superhydrophobic strain sensors for subtle human motion detection. Journal of Materials Science and Technology, 2022, 110, 35-42.	10.7	17
133	Liquid sensing properties of carbon black/polypropylene composite with a segregated conductive network. Sensors and Actuators A: Physical, 2014, 217, 13-20.	4.1	16
134	Dynamic chemical bonds design strategy for fabricating fast room-temperature healable dielectric elastomer with significantly improved actuation performance. Chemical Engineering Journal, 2022, 439, 135683.	12.7	16
135	Temperature and time dependence of electrical resistivity in an anisotropically conductive polymer composite with <i>in situ</i> conductive microfibrils. Journal of Applied Polymer Science, 2012, 124, 1808-1814.	2.6	15
136	Enhanced βâ€crystal formation of isotactic polypropylene under the combined effects of acidâ€corroded glass fiber and preshear. Polymer Composites, 2013, 34, 1250-1260.	4.6	15
137	Suppressing the skin–core structure in injection-molded HDPE parts via the combination of pre-shear and UHMWPE. RSC Advances, 2015, 5, 84483-84491.	3.6	15
138	Microribbon Structured Polyvinylidene Fluoride with High-Performance Piezoelectricity for Sensing Application. ACS Applied Polymer Materials, 2021, 3, 2411-2419.	4.4	15
139	Transcrystallization in nanofiber bundle/isotactic polypropylene composites: effect of matrix molecular weight. Colloid and Polymer Science, 2012, 290, 1157-1164.	2.1	14
140	Lightweight, mechanical robust foam with a herringbone-like porous structure for oil/water separation and filtering. Polymer Testing, 2018, 72, 86-93.	4.8	14
141	HDPE solution crystallization induced by electrospun PA66 nanofiber. Colloid and Polymer Science, 2011, 289, 843-848.	2.1	13
142	Superior actuation performance and healability achieved in a transparent, highly stretchable dielectric elastomer film. Journal of Materials Chemistry C, 2021, 9, 12239-12247.	5.5	13
143	Study of shear-induced interfacial crystallization in polymer-based composite through in situ monitoring interfacial shear stress. Journal of Materials Science, 2013, 48, 5354-5360.	3.7	12
144	Electrically conductive CB/PA6/HDPE composite with a CB particles coated electrospun PA6 fibrous network. Materials Letters, 2014, 114, 96-99.	2.6	12

#	Article	IF	CITATIONS
145	Tunable resistivity–temperature characteristics of an electrically conductive multi-walled carbon nanotubes/epoxy composite. Materials Letters, 2015, 159, 276-279.	2.6	12
146	Fabrication of a polymer/aligned shish-kebab composite: microstructure and mechanical properties. RSC Advances, 2015, 5, 60392-60400.	3.6	12
147	Mechanically Strengthened Polyamide 66 Nanofibers Bundles via Compositing With Polyvinyl Alcohol. Macromolecular Materials and Engineering, 2016, 301, 212-219.	3.6	12
148	Sandwiched film with reversibly switchable transparency through cyclic melting-crystallization. Chemical Engineering Journal, 2022, 442, 136205.	12.7	12
149	The Resistivity Response of an Anisotropically Conductive Polymer Composite with in-situ Conductive Microfibrils During Cooling. Polymer-Plastics Technology and Engineering, 2011, 50, 1511-1514.	1.9	10
150	Negative effect of stretching on the development of βâ€phase in βâ€nucleated isotactic polypropylene. Polymer International, 2011, 60, 1016-1023.	3.1	9
151	Tailoring microstructure and mechanical properties of injection molded isotactic–polypropylene via high temperature preshear. Polymer Engineering and Science, 2015, 55, 2714-2721.	3.1	9
152	Face-to-Face Assembly of Ag Nanoplates on Filter Papers for Pesticide Detection by Surface-Enhanced Raman Spectroscopy. Nanomaterials, 2022, 12, 1398.	4.1	9
153	Liquidâ€sensing behaviors of carbon black/polypropylene and carbon nanotubes/polypropylene composites: A comparative study. Polymer Composites, 2015, 36, 205-213.	4.6	8
154	Liquid-sensing behaviors of carbon black/polyamide 6/high-density polyethylene composite containing ultrafine conductive electrospun fibrous network. Colloid and Polymer Science, 2016, 294, 1343-1350.	2.1	8
155	Tunable temperature-resistivity behaviors of carbon black/polyamide 6 /high-density polyethylene composites with conductive electrospun PA6 fibrous network. Journal of Composite Materials, 2019, 53, 1897-1906.	2.4	8
156	Preparation of <scp>PVA</scp> / <scp>PAM</scp> /Ag strain sensor via compound gelation. Journal of Applied Polymer Science, 2022, 139, 51883.	2.6	8
157	Polymer microfibrillar tube for continuous oil/water separation and collection. Polymer, 2022, 239, 124440.	3.8	8
158	Multi-stimuli-responsive actuator based on bilayered thermoplastic film. Soft Matter, 2022, 18, 5052-5059.	2.7	8
159	The role of conductive pathways in the conductivity and rheological behavior of poly(methyl) Tj ETQq1 1 0.7843	14 <sub>.rg</sub> BT /C	overlock 10 T
160	Microstructure and Mechanical Properties of Isotactic Polypropylene Films Fabricated via Melt-Extrusion and Uniaxial-Stretching. Journal of Macromolecular Science - Physics, 2016, 55, 158-174.	1.0	6
161	Simultaneously improving tensile strength and toughness of meltâ€spun βâ€nucleated isotactic polypropylene fibers. Journal of Applied Polymer Science, 2016, 133, .	2.6	5
162	Alternating aligned conductive stripes in polypropylene film with remarkable anisotropy for sensing application. Sensors and Actuators B: Chemical, 2021, 330, 129370.	7.8	5

#	Article	lF	CITATIONS
163	Preparation of wearable strain sensor based on PVA/MWCNTs hydrogel composite. Materials Today Communications, 2022, 31, 103278.	1.9	5
164	Tribological Properties of Self-Lubricating Thermoplastic Polyurethane/Oil-Loaded Microcapsule Composites Based on Melt Processing. Industrial & Engineering Chemistry Research, 2021, 60, 16023-16031.	3.7	4
165	Farmingâ€Inspired Continuous Fabrication of Grating Flexible Transparent Film with Anisotropic Conductivity. Advanced Materials Technologies, 2022, 7, .	5.8	4
166	β-Crystal in the iPP melt encapsulated by transcrystallinity and spherulites: effect of molecular weight. Journal of Materials Science, 2013, 48, 2326-2333.	3.7	3
167	Organic liquid stimuliâ€response behaviors of electrically conductive microfibrillar composite with a selective conductive component distribution. Journal of Applied Polymer Science, 2012, 124, 4466-4474.	2.6	2
168	Comparative Study of Strain Sensing Behaviors of Carbon Black/Polypropylene and Carbon Nanotubes/Polypropylene with Different Tensile Speeds. Polymer-Plastics Technology and Engineering, 2013, 52, 1303-1307.	1.9	2
169	A Conductive Carbon Nanotube-Polymer Composite Based on a Co-continuous Blend. Journal of Macromolecular Science - Physics, 2013, 52, 167-177.	1.0	2
170	Revitalized βâ€form crystal during the remelting and recrystallization processes in isotactic polypropylene/glass fiber composites. Polymer Crystallization, 2018, 1, e10008.	0.8	2
171	Study on Impact Property and Fracture Morphology of Injection-molded Optical-grade Polycarbonate. Journal of Macromolecular Science - Physics, 2014, 53, 336-346.	1.0	1
172	Facile Fabrication of Nylon66/Multi-Wall Carbon Nanotubes/Polyvinyl Alcohol Nanofiber Bundles for Use as Humidity Sensors. Journal of Macromolecular Science - Physics, 2021, 60, 368-380.	1.0	1
173	Conductive Nanocomposites: Positive Temperature Coefficient (PTC) Evolution of Segregated Structural Conductive Polypropylene Nanocomposites with Visually Traceable Carbon Black Conductive Network (Adv. Mater. Interfaces 17/2017). Advanced Materials Interfaces, 2017, 4	3.7	0